RSC Advances

RSC Publishing

COMMUNICATION

View Article Online
View Journal | View Issue

Development of a multifunctional catalyst for a ''relay'' reaction†

Cite this: *RSC Advances*, 2013, **3**, 2186

Received 9th November 2012,
Accepted 6th December 2012

DOI: 10.1039/c2ra22829g

www.rsc.org/advances

Anal Kr. Ganai,[ab] Pravin Shinde,[a] Basab B. Dhar,[b] Sayam Sen Gupta*[b] and B. L. V. Prasad*[a]

In the area of catalysis, nanoparticles and enzymes are two of the most important systems. By amalgamating the two, we present here proof of the concept that it is possible to prepare a multifunctional catalyst that can carry out a ''relay'' reaction. The catalyst consists of a surface bound enzyme on a $metal_{core}$–$silica_{shell}$ nanoparticle architecture. Here the enzyme catalyzes the 1st reaction and the metal nanoparticles act as a catalyst for the 2nd reaction of the product from the 1st reaction. In particular, we have studied the catalytic activity of glucosidase grafted $Au@mSiO_2$ on 4-nitrophenyl-β-glucopyranoside, where glucosidase will catalyse the 1st step to generate 4-nitrophenol, which acts as a substrate for the next reduction step which is catalysed by the Au nanoparticles present inside the mesoporous silica shell.

Living cells represent a perfect chemical factory where nutrients are converted into the complex chemical building blocks needed for the cells' metabolism.[1,2] The multistep synthesis of metabolites occurs *via* a series of sequential reactions catalyzed by enzymes in which the product of one reaction serves as a substrate for the subsequent reaction. Such examples of multienzymatic systems are observed in numerous biosynthetic pathways such as in polyketide biosysnthesis.[3,4] These metabolic pathways serve as an inspiration for chemists to develop similar synthetic systems so that a multistep organic synthesis of a desired compound can be performed in one pot without the isolation of the intermediates.[5] However, mimicking the living cell is still a distant goal for synthetic chemists. Currently, reaction cascades that combine two or more catalytic transformations in a tandem or one-pot process are being increasingly used and have proven to be a viable synthetic route for many organic compounds.[6] The big advantage of such systems lies in the fact that multiple catalysts operating in tandem eliminate the time and yield losses associated with the isolation and purification of intermediates in multistep sequences.[7] Hence a lot of effort has been directed towards the development of such concurrent tandem catalytic systems.[5] We would like to note here that most of the efforts in this direction have been focused towards the development of tandem catalytic systems based on organometallic complexes.[8] On the other hand, catalysis using enzymes is becoming increasingly important because they offer high stereo specificity and unparalleled selectivity to chemical reactions under mild conditions, such as neutral pH and room temperature in water.[9,10] However, the types of chemical reactions catalyzed by enzymes are limited compared to the vast repertoire of chemical transformations developed using transition metals as catalysts (including organotransition metal complexes and recently metal nanoparticles).[11–15] In this context we envisaged that the coupling of an enzymatic reaction with a transition metal catalyzed reaction in a tandem fashion can open up new frontiers in organic transformation. Considerable efforts have been made in this direction to immobilize enzymes/biocatalysts onto mesoporous supports using different strategies and these have been reviewed recently;[16] although we would like to note here that the examples where metal nanoparticles and enzymes are immobilized onto a single host so that both of these act as catalysts to bring about cascade reactions are rather sparse.[17] As one would expect, the development of such intricate systems is laden with several major challenges. First, the metal catalyst and the enzyme should be incorporated into a matrix in such a way that the metal catalyst does not interact with the plethora of functional groups present in the enzyme thereby denaturating it, leading to activity loss.[18] Secondly, we should be able to recover both the enzyme and the metal nanoparticles, ensuring that the metal and enzyme are not leached into the reaction mixture.[19,20] The metal would also need to have an appropriate surface passivation such that their aggregation during the reaction is prevented.[21–23] Finally both the enzymes and the nanoparticles should be easily accessible to the substrates. One way to overcome all these challenges would be to incorporate both the metal catalyst and enzyme in a heterogeneous support [24–28] in such a manner that they do not interact with each other, yet are accessible to small organic molecules.[29–31]

[a]*Materials Chemistry Division; National Chemical Laboratory, Pune 411008*
[b]*Chemical Engineering and Process Development Division; National Chemical Laboratory, Pune 411008. E-mail: ss.sengupta@ncl.res.in; pl.bhagavatula@ncl.res.in*

† Electronic supplementary information (ESI) available: Experimental details concerning particle synthesis and characterization. See DOI: 10.1039/c2ra22829g

We hereby report the design and synthesis of mesoporous silica nanoparticles ($mSiO_2$) coated on gold nanoparticles in a core–shell architechture with an enzyme grafted onto the outside silica surface. To the best of our knowledge, this is the first example where a functional enzyme has been covalently attached to the surface of a $Au_{core}mSiO_{2shell}$ ($Au@mSiO_2$) construct which allows a two step reaction to be carried out by the enzyme and metal NPs either independently or cooperatively without interference between the two.[32–34] The following features of the hybrid material make it very attractive. (i) The synthesis of Au nanoparticles encapsulated in MSN is performed by a simple one-pot procedure onto the external surface of which enzymes can be grafted easily. (ii) This hybrid material allows two concurrent reactions to be carried out in tandem such that the product released by the first reaction becomes the substrate for the second reaction. This can be compared to a "relay" race where the performance of the second participant depends upon the first. (iii) At the end of the reaction the hybrid MSN can be separated by simple centrifugation and subsequently reused. As a proof of concept, a cascade reaction was carried out where the first step involved the hydrolysis of 4-nitrophenyl-β-glucopyranoside by the enzyme glucosidase that was anchored on the external surface of MSN. In the subsequent step, the 4-nitrophenol released from the first reaction diffuses inside the pores of MSN where it is reduced to the corresponding amine by the gold nanoparticle in the presence of $NaBH_4$.[35,36] The detailed kinetics of both the reaction steps is also discussed.

Our strategy to synthesize the enzyme grafted hybrid material involves three steps (Scheme 1, for full details of the synthesis please see the ESI†). The first step in this endeavour was the synthesis of $Au@mSiO_2$ nanoparticles. In the second step, epoxide was grafted onto the outside surface of these particles using general silane chemistries. Finally, β-glucosidase was immobilized by the ring opening of the epoxide by the NH_2 groups of lysine present in β-glucosidase to prepare the hybrid catalyst, $Au@mSiO_2$@glucosidase.

The core shell nanoparticles ($Au@mSiO_2$) were synthesized using a sol–gel procedure with the preformed Au nanoparticles. Au nanoparticles of ~8 nm (please see ESI Fig. 1†) size were prepared by the borohydride reduction of $HAuCl_4$. To prepare the silica shell on the Au nanoparticles, we used a typical Stober method. The nanoparticles were treated with the ionic surfactant cetyltrimethylammonium bromide (CTAB). CTAB serves not only as a stabilizing surfactant for Au nanocrystals in the aqueous phase but also as the organic template for the formation of mesopores in the sol–gel reaction.[37] The resulting core–shell nanoparticles were separated by centrifugation, redispersed in ethanol, and then characterized by transmission electron microscopy. From TEM analysis, the size of the particles was determined to be ~42 nm (Fig. 1A). After silica coating, it has been observed that the particles were well dispersed in water.

Finally, the CTAB template was removed from the as-synthesized material by refluxing with ethanol. This led to the opening of pores in the silica matrix and the formation of $Au@mSiO_2$ particles (Fig. 1B). The particles were found to be well separated from each other and the size distribution remained the same as that observed before the CTAB removal (Fig. 1C). The bare Au nanoparticles displayed a UV-Vis absorption band at 520 nm (Fig. 2B), which is characteristic of the plasmon resonance bands of spherical gold nanoparticles. After the silica encapsulation, the

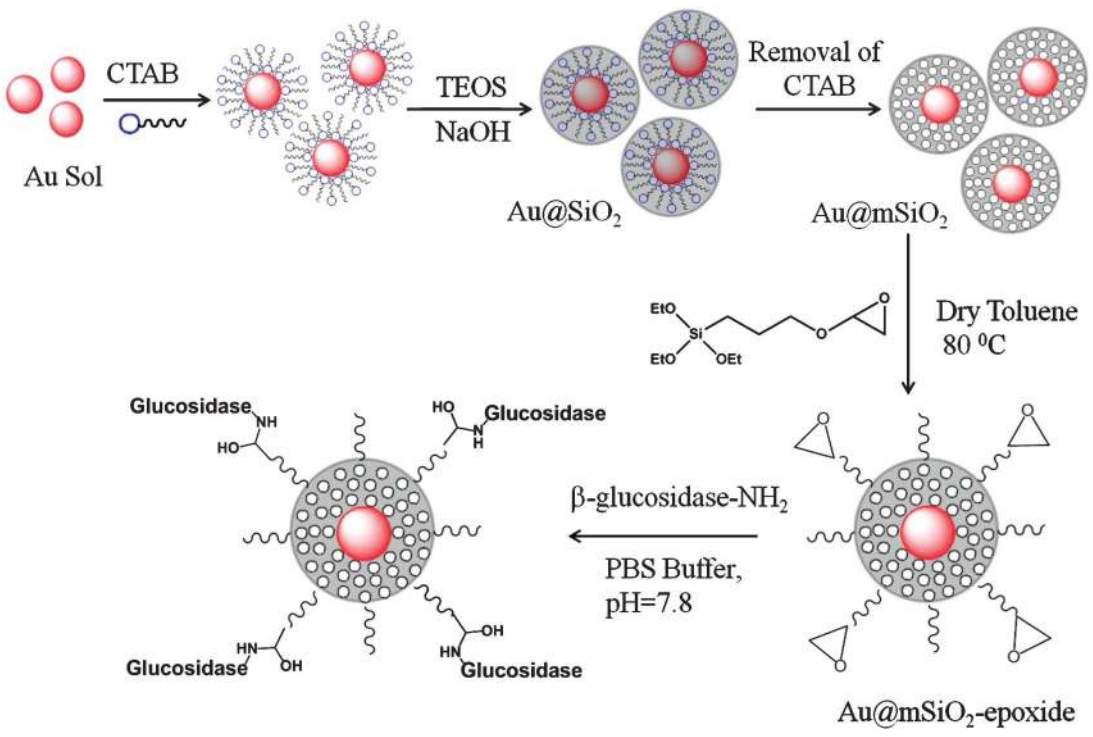

Scheme 1 Schematic illustrations of the synthetic procedure for gold nanocrystal/mesoporous silica core shell nanoparticles.

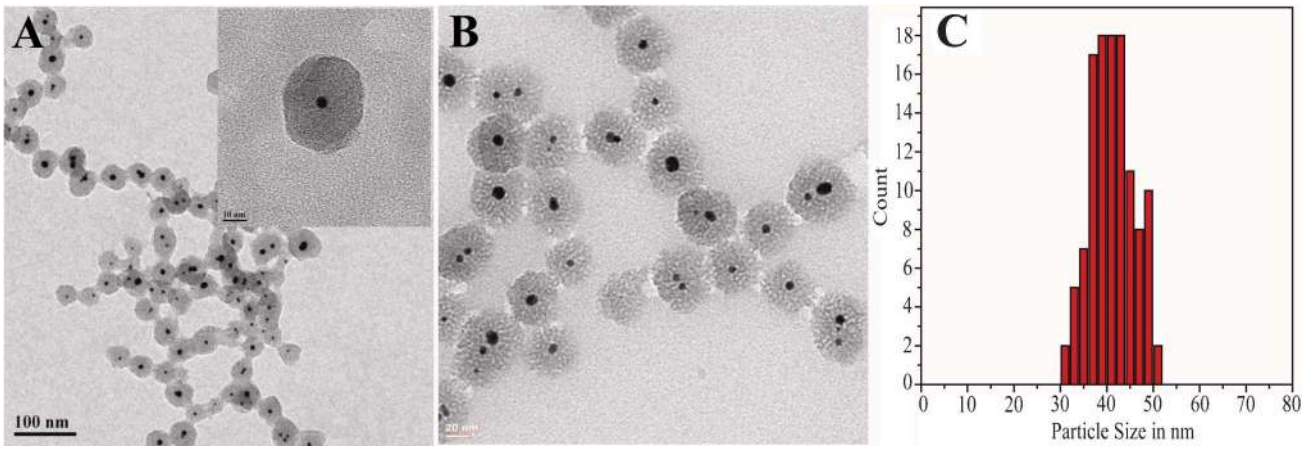

Fig. 1 TEM images of core–shell mesoporous silica NPs. (A) As synthesized Au@SiO_2 nanoparticles. (B) Au@mSiO_2 particles after removal of CTAB. (C) Size distribution of the particles.

peak shifted from 520 to 533 nm (Fig. 2A), which can be attributed to the coating of the silica shell, which changes the effective dielectric constant (Fig. 2A).[38] The formation of metallic gold nanoparticles was also confirmed by the X-ray powder diffraction (XRD) pattern. The wide-angle XRD pattern of mesoporous silica coated Au nanopaticles obtained with Cu-Kα (Fig. 2B) shows four Au diffraction peaks at $2\theta \approx 38.1^\circ$, 44.4°, 64.6° and 76.6°. These can be assigned to (111), (200), (220), and (311) reflections of the cubic (fcc) gold lattice (JCPDS card No. 04–0784) respectively.[20] Furthermore, a very broad signal at $2\theta = 22.31^\circ$ suggests the presence of amorphous silica. The average particle size of the metal core calculated by the Scherrer equation using the half width of the intense (111) reflection was ~8 nm, which is comparable with the value obtained from the TEM images. To further investigate the chemical composition of the materials, X-ray photoelectron spectroscopy (XPS), was performed (Fig. 2C).

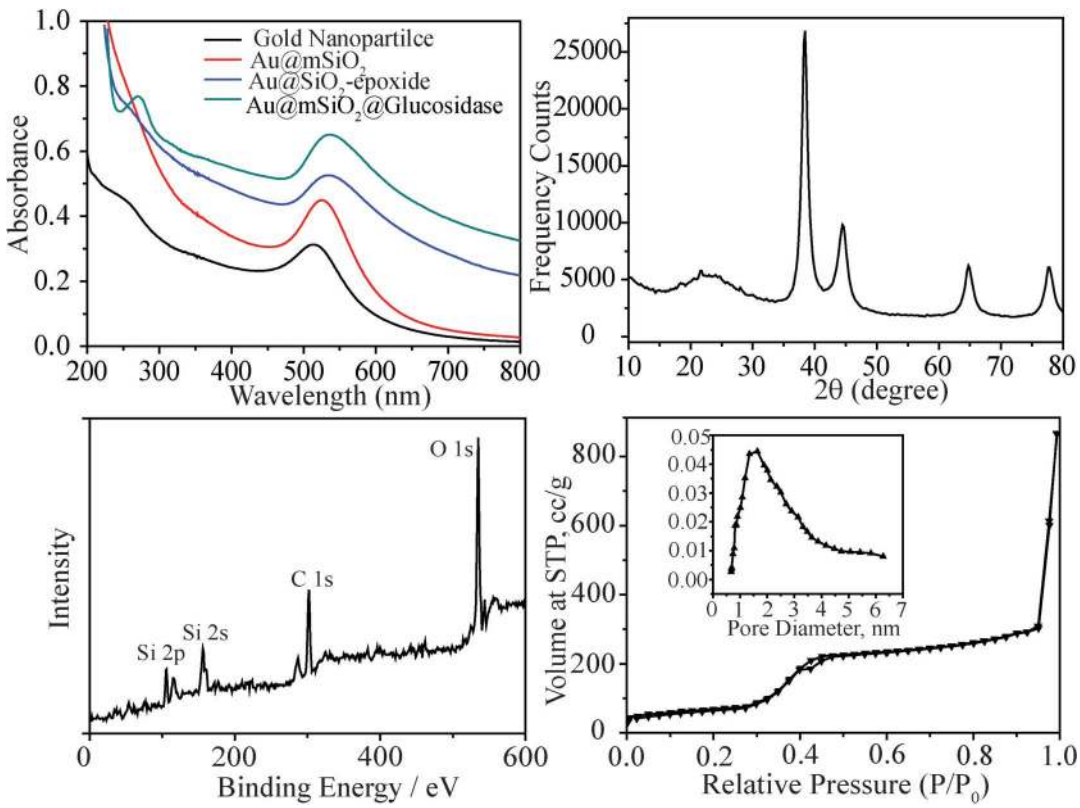

Fig. 2 (A) Wide-angle XRD pattern of Au@mSiO_2 particles. (B) UV-Vis spectra of Au, Au@SiO_2, Au@mSiO_2 and Au@mSiO_2-Glucosidase NPs. (C) N_2 adsorption/desorption isotherms (inset: pore size distribution from adsorption branch). (D) XPS spectrum of Au@mSiO_2 NPs.

We did not observe any peaks of Au at 84.57 eV and 88.21 eV for Au $4f_{7/2}$ and Au $4f_{5/2}$. Since the typical detection depth of XPS is 10 nm, the absence of peaks from metallic gold suggests that all the Au particles are covered with silica.[29] Atomic Absorption Spectroscopy (AAS) was applied to study the content of gold per gram of Au@mSiO$_2$. The weight% of gold was determined to be 33.5%. N_2 adsorption/desorption isotherms (Fig. 2D) show a BET surface area of 381 $m^2\ g^{-1}$ and the corresponding BJH pore size distribution (inset of Fig. 2C) demonstrates that Au@mSiO$_2$ has well-developed mesopores with an average size of 1.6 nm. This nitrogen-sorption analysis showed that the cavity of the mesoporous SiO_2 was accessible to N_2 molecules, which may allow other guest molecules to diffuse into the hollow cavities.[27] The pore volume was determined to be 1.19 $cm^3\ g^{-1}$. Assuming that the removal of CTAB leaves a straight pore and based on the initial size of the bare Au NPs and the thickness of silica shell formed we can deduce the pore depth to be $\sim$17 nm.

The grafting of the epoxide functional group was done using well established silane chemistry.[25] Au@mSiO$_2$ nanoparticles were treated with (3-glycidyloxypropyl)trimethoxysilane in dry toluene for 16 h at 80 °C. After washing three times with ethanol, the material was characterized with infra-red spectroscopy (Fig. 3A and ESI Fig. 2†) and thermogravimetric analysis (TGA) in the presence of air (Fig. 3B). From the IR spectra, it was observed that the peak intensity at 3000 cm^{-1} corresponding to the stretching frequency of $-CH_2$ had increased, indicating the incorporation of glycidyl groups onto the surface. The successful grafting of the epoxide was further characterized by TGA. A weight loss of nearly 20% was observed after grafting with (3-glycidyloxypropyl) trimethoxysilane, which is due to the combustion of the organic moiety present on the surface of Au@mSiO$_2$. The epoxide grafting density as determined from TGA analysis was $\sim$1.8 mmol g^{-1} of sample.

The epoxy grafted Au@mSiO$_2$ nanoparticles were reacted with β-glucosidase in PBS buffer (pH = 7.8, 0.1 mM) so that the amino groups of lysine in β-glucosidase induces ring-opening of the epoxy group on the surface of Au@mSiO$_2$, leading to the covalent immobilization of the enzyme on the surface of the nanoparticle (Au@mSiO$_2$@glucosidase). After the completion of the reaction, the material was washed with buffer solution several times until the supernatant showed no UV absorption characteristic of the enzyme. Control experiments were performed so that no enzymes were electrostatically attached onto the Au@mSiO$_2$ nanoparticle surface. First, the β-glucosidase grafted Au@mSiO$_2$ was washed with NaCl (0.1 M) to destabilize the electrostatic attraction between the nanoparticle surface and the non-covalently bound enzymes so that they could be washed out easily.[39] Since no enzymes were observed in the supernatant during these washings, we concluded that our synthetic procedure leads to the covalent attachment of the enzyme to the nanoparticle surface and that any of the non-covalently bound enzymes get washed away during the purification. Secondly, the incubation of β-glucosidase with bare Au@mSiO$_2$ (particles that did not have the epoxide group grafted on them) did not show any attachment of the enzyme onto the nanoparticle surface. The Au@mSiO$_2$@glucosidase nanoparticles displayed UV-Vis absorption bands at 520 nm and 270 nm (Fig. 2B), which are characteristic of the plasmon resonance bands of spherical gold nanoparticles and glucosidase enzymes, respectively. The amount of grafted enzyme was estimated to be about 1.7×10^{-6} mol g^{-1} of Au@mSiO$_2$@glucosidase core–shell nanoparticles which corresponds to about 23% by weight of the Au@mSiO$_2$@glucosidae nanoparticles. The amount of enzyme was estimated from TGA analysis to be 1.15×10^{-6} mol g^{-1} (Fig. 3B). Since the pore size of the Au@mSiO$_2$ nanoparticle (1.6 nm) was less than the average diameter of the enzyme, there was no possibility that the enzyme would be immobilized inside the pores of the nanoparticle.

The activities of the immobilized bifunctional catalyst Au@mSiO$_2$@glucosidase was tested in a tandem sequence involving the hydrolysis of 4-nitrophenyl-β-glucopyranoside to 4-nitrophenol and the subsequent reduction of 4-nitrophenol to 4-aminophenol (Scheme 2). First, 4-nitrophenyl-β-glucopyranoside was added to Au@mSiO$_2$@glucosidase to initiate its efficient hydrolysis to the corresponding 4-nitrophenol by the immobilized β-glucosidase on the silica surface. The kinetics of this hydrolysis reaction were studied by UV-Vis spectroscopy. The gradual increase in the peak height at 400 nm with time indicated the formation of 4-nitrophenol. The absorbance *vs.* time data for this

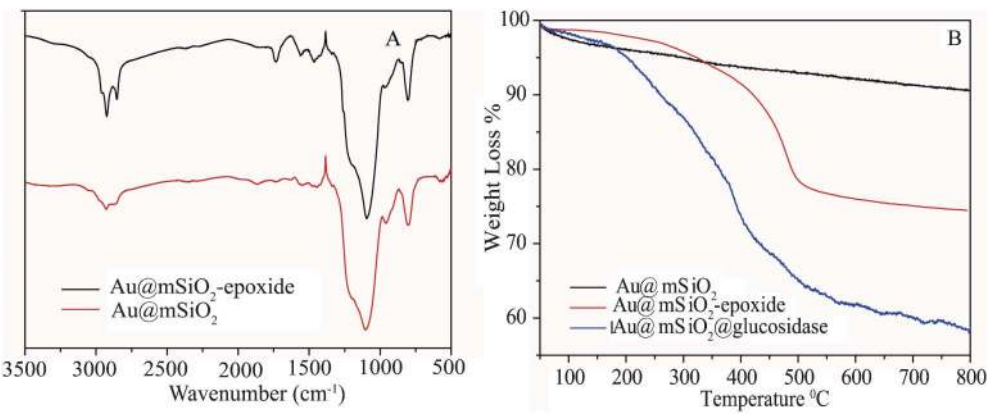

Fig. 3 (A) IR spectra and (B) TGA of Au@mSiO$_2$ and Au@SiO$_2$-epoxide nanoparticles.

Scheme 2 The schematic illustration of tandem reaction using enzyme conjugated Au@mSiO$_2$ nanoparticles.

particular reaction was fitted according to the first order equation $A_t = A_o e^{-kt}$, where A_o and A_t stand for absorbance at time, $t = 0$ and t min, respectively (ESI Fig. 3,† first reaction) and the rate constant k was determined to be 4.16×10^{-2} min^{-1} ($R^2 = 0.9996$).

After the completion of the hydrolysis reaction, excess NaBH$_4$ was added to the reaction mixture so that the gold core present inside the nanoparticle could reduce the 4-nitrophenol generated by the previous reaction into the corresponding 4-aminophenol. The presence of pores in the silica coated Au nanoparticle allows both the 4-nitrophenol and NaBH$_4$ to diffuse through the pores to the surface of the Au nanoparticle, where the subsequent reduction reaction takes place. A control reaction performed with porous silica nanoparticles without any Au nanoparticles embedded inside showed no reaction over 24 h, indicating that the presence of the gold nanoparticle as a catalyst is essential for this reaction. The kinetics of the 4-nitrophenol reduction in the presence of Au@mSiO$_2$@glucosidase was studied by UV-Vis spectroscopy (Fig. 4).

After the addition of NaBH$_4$, it was found that the peak height at 400 nm gradually decreased with time. The decrease in peak intensity at 400 nm with time can be used to calculate the rate constant of this reduction reaction. The ratio of C_t to C_0, where C_t is the concentration of 4-nitrophenol at time, t, and C_0 is the initial 4-nitrophenol concentration, was determined from that of the respective absorbance ratio (A_t/A_o) at 410 nm. This reaction follows first order kinetics with a rate constant of 3.0×10^{-1} min^{-1} which was obtained from $\ln(A_t - A_{infi})$ *vs.* time plot (ESI Fig. 3,† second reaction) as well as the absorbance *vs.* time plot considering the rate equation $A_t = A_o e^{-kt}$. Hence we were able to perform two reactions in tandem in a one-pot sequence using our Au@mSiO$_2$@glucosidase nanoparticles. We were also able to recover the Au@mSiO$_2$@glucosidase nanoparticle by simple centrifugation after the completion of the reactions. We then attempted to check if Au@mSiO$_2$@glucosidase nanoparticles could be recycled for more catalytic cycles. Although Au@mSiO$_2$@glucosidase nanoparticles were able the carry both the hydrolysis reaction and the subsequent reduction reaction independently for 5 catalytic cycles, the activity for cascade reactions rapidly decreased in successive cycles (ESI Fig. 4†). We

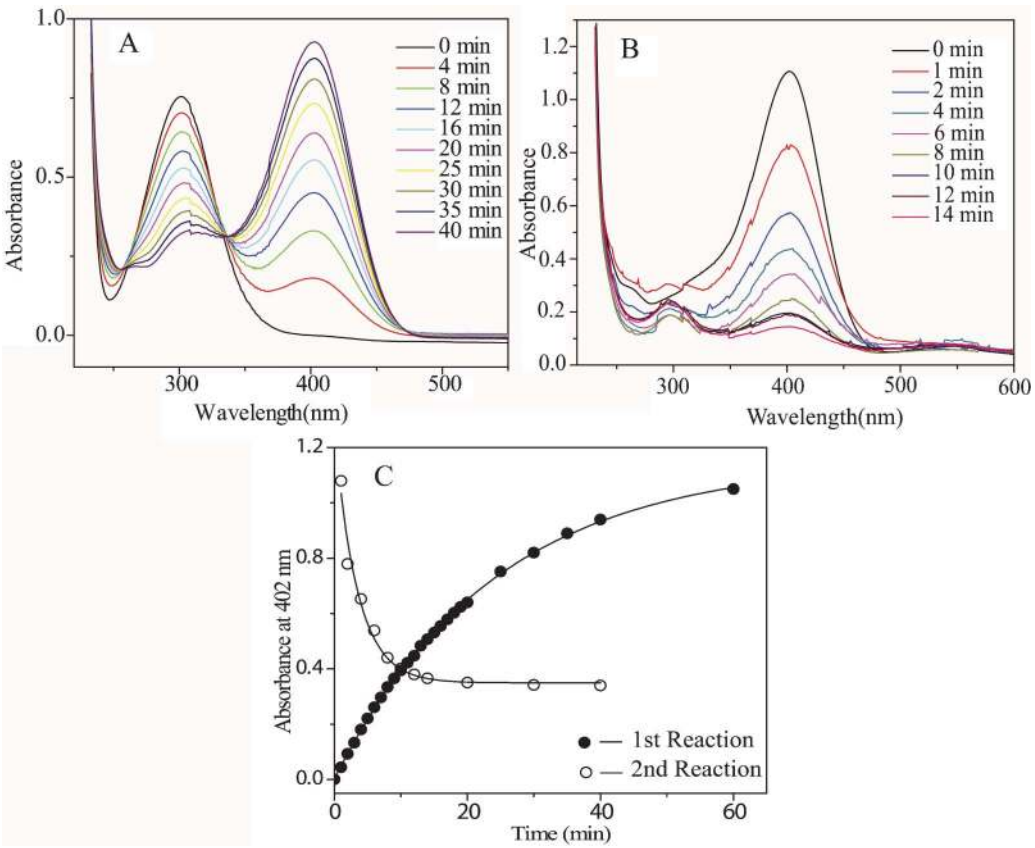

Fig. 4 (A) Time-dependent UV-vis absorption spectral changes of the 1st reaction mixture catalyzed by Au@mSiO2@glucosidase. (B) Time-dependent UV-vis absorption spectral changes of the 2nd reaction mixture catalyzed by enzyme Au@mSiO2@glucosidase. (C) Combined plot for the exponential change of OD.

attributed this to the possibility of $NaBH_4$ denaturing the enzyme because of the very high pH generated by the hydrolysis of $NaBH_4$.

In conclusion, we successfully demonstrated the construction of a bifunctional "relay" catalyst that could carry out a sequential two step reaction. Au nanoparticles were successfully encapsulated inside a mesoporous silica shell followed by enzyme immobilization on the surface of the shell. In addition, the catalytic activity of these materials was tested using a model reaction, where the product released by the first reaction becomes the substrate for the second reaction. This study also indicates that the micropores in the silica shell could allow the transport of small species into the cavity. Moreover, this strategy may be easily extended to encapsulate other metal NPs inside the mesoporous silica shell and to functionalize the silica surface with a desirable chemical moiety using well established silane chemistry.

Acknowledgements

AKG and PS acknowledge CSIR, New Delhi, India and UGC, India respectively for fellowships. B. B. D. acknowledges CSIR (New Delhi) for an associateship. SSG acknowledges DST, New Delhi (Grant No.: SR/S1/PC-56/2008) for funding.

References

1 Y. Chi, S. T. Scroggins and J. M. J. Fréchet, *J. Am. Chem. Soc.*, 2008, **130**, 6322.
2 D. M. Vriezema, P. M. L. Garcia, N. Sancho Oltra, N. S. Hatzakis, S. M. Kuiper, R. J. M. Nolte, A. E. Rowan and J. C. M. van Hest, *Angew. Chem., Int. Ed.*, 2007, **46**, 7378.
3 C. Khosla, *Chem. Rev.*, 1997, **97**, 2577.
4 J. Staunton and B. Wilkinson, *Chem. Rev.*, 1997, **97**, 2611.
5 J.-C. Wasilke, S. J. Obrey, R. T. Baker and G. C. Bazan, *Chem. Rev.*, 2005, **105**, 1001.
6 A. Bruggink, R. Schoevaart and T. Kieboom, *Org. Process Res. Dev.*, 2003, **7**, 622.
7 B. M. Trost, *Angew. Chem., Int. Ed. Engl.*, 1995, **34**, 259.
8 M. Asikainen and N. Krause, *Adv. Synth. Catal.*, 2009, **351**, 2305.
9 P. Jochems, Y. Satyawali, L. Diels and W. Dejonghe, *Green Chem.*, 2011, **13**, 1609.
10 U. T. Bornscheuer, *Angew. Chem., Int. Ed.*, 2003, **42**, 3336.
11 C. H. Christensen and J. K. Nørskov, *Science*, 2010, **327**, 278.
12 E. García-Urdiales, I. Alfonso and V. Gotor, *Chem. Rev.*, 2005, **105**, 313.
13 P. Hervés, M. Pérez-Lorenzo, L. M. Liz-Marzán, J. Dzubiella, Y. Lu and M. Ballauff, *Chem. Soc. Rev.*, 2012, **41**, 5577.
14 L. Veum and U. Hanefeld, *Chem. Commun.*, **2006**, 825.
15 M. Stratakis and H. Garcia, *Chem. Rev.*, 2012, **11**, 4469.
16 M. Hartmann and D. Jung, *J. Mater. Chem.*, 2010, **20**, 844–857.
17 P. Maki-Arvela, S. Sahin, N. Kumar, T. Heikkila, V.-P. Lehto, T. Salmi and D. Y. Murzin, *J. Mol. Catal. A: Chem.*, 2008, **285**, 132.
18 K. M. Polizzi, A. S. Bommarius, J. M. Broering and J. F. Chaparro-Riggers, *Curr. Opin. Chem. Biol.*, 2007, **11**, 220.
19 D. Astruc, F. Lu and J. R. Aranzaes, *Angew. Chem., Int. Ed.*, 2005, **44**, 7852.
20 Y. Wang and F. Caruso, *Chem. Mater.*, 2005, **17**, 953.
21 X. Du and J. He, *Nanoscale*, 2012, **4**, 852.
22 S. Liu and M.-Y. Han, *Chem. Asian J.*, 2010, **5**, 36.
23 E. Lam, S. Hrapovic, E. Majid, J. H. Chong and J. H. T. Luong, *Nanoscale*, 2012, **4**, 997.
24 P. Botella, A. Corma and M. T. Navarro, *Chem. Mater.*, 2007, **19**, 1979.
25 N. Brun, A. Babeau Garcia, H. Deleuze, M. F. Achard, C. Sanchez, F. Durand, V. Oestreicher and R. Backov, *Chem. Mater.*, 2010, **22**, 4555.
26 D. Brady and J. Jordaan, *Biotechnol. Lett.*, 2009, **31**, 1639.
27 S. Wang, M. Zhang and W. Zhang, *ACS Catal.*, 2011, **1**, 207.
28 J. Han, P. Fang, W. Jiang, L. Li and R. Guo, *Langmuir*, 2012, **28**, 4768.
29 X. Fang, Z. Liu, M.-F. Hsieh, M. Chen, P. Liu, C. Chen and N. Zheng, *ACS Nano*, 2012, **6**, 4434.
30 L. Tan, D. Chen, H. Liu and F. Tang, *Adv. Mater.*, 2010, **22**, 4885.
31 S. Wu, J. Dzubiella, J. Kaiser, M. Drechsler, X. Guo, M. Ballauff and Y. Lu, *Angew. Chem., Int. Ed.*, 2012, **51**, 2229.
32 E. L. Margelefsky, R. K. Zeidan and M. E. Davis, *Chem. Soc. Rev.*, 2008, **37**, 1118.
33 R. K. Zeidan, S.-J. Hwang and M. E. Davis, *Angew. Chem.*, 2006, **118**, 6480.
34 Y. Huang, S. Xu and V. S. Y. Lin, *Angew. Chem., Int. Ed.*, 2011, **50**, 661.
35 S. Carregal-Romero, N. J. Buurma, J. Pérez-Juste, L. M. Liz-Marzán and P. Hervés, *Chem. Mater.*, 2010, **22**, 3051.
36 J. Lee, J. C. Park, J. U. Bang and H. Song, *Chem. Mater.*, 2008, **20**, 5839.
37 J. Kim, H. S. Kim, N. Lee, T. Kim, H. Kim, T. Yu, I. C. Song, W. K. Moon and T. Hyeon, *Angew. Chem.*, 2008, **120**, 8566.
38 Y. J. Wong, L. Zhu, W. S. Teo, Y. W. Tan, Y. Yang, C. Wang and H. Chen, *J. Am. Chem. Soc.*, 2011, **133**, 11422.
39 R. K. Singh, Y.-W. Zhang, N.-P.-T. Nguyen, M. Jeya and J.-K. Lee, *Appl. Microbiol. Biotechnol.*, 2011, **89**, 337.